



HAL
open science

New Results From the 2021 FEEDELIO Experiment - a Focus on Reciprocity

Perrine Lognone, Aurélie Montmerle Bonnefois, Jean-Marc Conan, Laurie Paillier, Cyril Petit, Caroline Lim, Serge Meimon, Joseph Montri, Jean-Francois Sauvage, Nicolas Vedrenne

► **To cite this version:**

Perrine Lognone, Aurélie Montmerle Bonnefois, Jean-Marc Conan, Laurie Paillier, Cyril Petit, et al.. New Results From the 2021 FEEDELIO Experiment - a Focus on Reciprocity. IEEE, pp.261-266, 2022, 10.1109/ICSOS53063.2022.9749723 . hal-03646974

HAL Id: hal-03646974

<https://hal.science/hal-03646974>

Submitted on 20 Apr 2022

HAL is a multi-disciplinary open access archive for the deposit and dissemination of scientific research documents, whether they are published or not. The documents may come from teaching and research institutions in France or abroad, or from public or private research centers.

L'archive ouverte pluridisciplinaire **HAL**, est destinée au dépôt et à la diffusion de documents scientifiques de niveau recherche, publiés ou non, émanant des établissements d'enseignement et de recherche français ou étrangers, des laboratoires publics ou privés.

New Results From the 2021 FEEDELIO Experiment – a Focus on Reciprocity

Perrine Lognoné^{*†}, Aurélie Montmerle Bonnefois^{*}, Jean-Marc Conan^{*}, Laurie Paillier^{*}, Cyril Petit^{*}, Caroline B. Lim^{*†}, Serge Meimon^{*}, Joseph Montri^{*}, Jean-François Sauvage^{*}, Nicolas Védrenne^{*}

^{*}ONERA, DOTA, Paris Saclay University
92322 Châtillon, FRANCE
Email: perrine.lognone@onera.fr
[†]Télécom Paris
91120 Palaiseau, FRANCE

Abstract—The FEEDELIO experiment aims at demonstrating adaptive optics capability to mitigate the atmospheric turbulence channel disturbances in a GEO-Feeder relevant environment. In addition to the bi-directional data acquired in presence of anisoplanatism, this measurement campaign was an opportunity to assess the optical quality of the bench and to improve calibration procedures. To this end, we conducted a reciprocity experiment. We measured a channel reciprocity up to 95% and identified, through numerical simulations, that residual non common path aberrations were the primary source limiting the effective reciprocity.

Index Terms—adaptive optics, reciprocity, optical feeder links, NCPAs

I. INTRODUCTION

In order to address the increasing need for very high throughput data links between ground and geostationary satellites, optical technologies are a very competitive candidate. However, their future depends on the ability to overcome channel disruptions and large link budget losses caused by the optical propagation through the turbulent atmosphere.

In 2019, the first FEEDELIO experiment, which consisted in a 13 km slant path optical link in Tenerife, proved the feasibility of adaptive optics (AO) pre-compensation of optical links in an environment whose properties are similar to a GEO feeder link. It also demonstrated significant gain in the link budget, as well as significant signal fluctuation reductions, compared to both uncompensated and tip-tilt only corrected beam [1] [2].

We conducted in October 2021 a second FEEDELIO experiment, with the aim of acquiring new time series in a wider variety of turbulence conditions. We took this opportunity to implement improved calibration procedures. In particular, we performed a reciprocity experiment in order to demonstrate the link reciprocity over the FEEDELIO link geometry and to assess the calibration quality.

The reciprocity principle, introduced by Shapiro [3], has been largely demonstrated in the framework of free space

optics (FSO) horizontal links [4] [5], with the motivation to obtain real-time knowledge on the telecommunication channel state (see [6] and references therein). However, to our knowledge, it has not been demonstrated in an asymmetrical system configuration equipped with AO, as in the FEEDELIO demonstration.

We therefore present in this paper the results of the reciprocity experiment performed during this measurement campaign. Quasi-reciprocal time series have been obtained with a co-axial bi-directional 9 modes corrected/pre-compensated link with a correlation coefficient up to 95%. We show that the remaining 5% are in accordance with the decorrelation induced by the residual non-common path aberrations (NCPAs). The impact of these NCPAs is evaluated through numerical simulations thanks to in house end-to-end (E2E) models. We will then discuss how this reciprocity experiment can be used for calibration and simulation purposes.

II. FEEDELIO EXPERIMENT

A. Overview of the experiment

The aim of the FEEDELIO experiment is to demonstrate the effectiveness of an AO pre-compensated optical link in improving the telecom link budget in presence of point-ahead angle (PAA) induced anisoplanatism in conditions representative of a GEO-Feeder link.

The experiment took place in Tenerife, Canary Island, hosted at the ESA premises. A two week first measurement campaign occurred in April 2019 and a two week second measurement campaign took place in October 2021 in order to gather additional data. The optical link was established between ESA's optical ground station (OGS) dome and the top of the mount Teide on a 13.2 km 5° elevation slant path [7].

To emulate the GEO-Feeder link, two terminals were designed :

- The satellite terminal breadboard (STB) to emulate the satellite.

This terminal is composed of two modules, one on-axis and the other off-axis as to emulate PAA, on the top

[†]Currently working at : LNE-SYRTE, Observatoire de Paris, Université PSL, CNRS, Sorbonne Université, 75014 Paris, FRANCE



Fig. 1. Picture of the 13.2 km line of sight between the OGS Dome (GTB) and the satellite emulator on top of the Teide mountain (STB). Credits Geraldine Artaud (CNES).

of the mount Teide as depicted in Fig. 1. In the frame of this reciprocity experiment we will focus on the on-axis module. It provides the reference downlink beacon at 1550 nm and is also equipped with a receiver to allow for the reciprocity experiment. The entrance pupil has a small 1.8 mm diameter and the receiver is a low noise PIN 20 kHz photodiode.

- The ground terminal breadboard (GTB) to emulate the OGS.

The GTB is composed of a 35 cm diameter commercial telescope and an optical bench that receives the downlink beacon, performs the AO correction on the downlink and pre-compensates the uplink. The uplink optical path is equipped with a point ahead mirror (PAM). The downlink signal is coupled to a single mode fiber (SMF) after the AO system. The signal is then detected by a low noise PIN 20 kHz photodiode.

This AO system is composed of an Alpao 95-17 deformable mirror (DM), a wavefront sensor (WFS) equipped with a Raptor Owl HS camera and a Shakti real-time computer. The WFS has 8x8 sub-apertures, the DM has 11x11 actuators, and the AO system runs at 1.5 kHz with a 2.3 frames delay. More details on the AO loop performance can be found in [8].

B. Upgrades of the second campaign

The first campaign was successful and the results as well as their analysis are to be published [2]. However, due to poor weather conditions, the amount of data was limited. As a result, the objective of this second campaign was to acquire a large amount of data in various turbulent conditions (various anisoplanatic, phase disturbance and scintillation regimes).

In addition, this second campaign was an opportunity to improve the bench and measurement procedures. The following upgrades were implemented :

- Finer radiometric calibration.

- Finer environment estimation parameters tools. In addition to the profilometry tools already available [9], a wind speed parameter estimator was implemented. The method relies on the analysis of the log-amplitude temporal spectrum [10].
- Upgrade of the reciprocity set-up.

III. A FOCUS ON THE RECIPROCITY EXPERIMENT

A. Aim, set-up and data acquisition protocol

The reciprocity experiment aimed at demonstrating the coupling flux reciprocity in a GEO-Feeder like scheme, equipped with an AO system. To that end, an AO corrected bidirectional link was established between the on-axis STB module and the GTB module. The measurement protocol consisted in simultaneously acquiring the AO corrected downlink signal in the GTB and pre-compensated on-axis uplink signal in the STB. Three types of AO corrections (Tip-Tilt, 9 modes, full-correction) are applied for each acquisition and each sub-acquisition is 10 s long. We recall that the sampling frequency of the PIN photodiodes is 20 kHz.

B. Reciprocity performance metric

To evaluate the reciprocity of the coupled flux time series f_{STB} and f_{GTB} , we compute the Pearson correlation coefficient (PCC) [11] which is defined as :

$$\text{PCC}_{f_{\text{STB}}, f_{\text{GTB}}} = \frac{\text{COV}(f_{\text{STB}}, f_{\text{GTB}})}{\sigma_{f_{\text{STB}}} \sigma_{f_{\text{GTB}}}} \quad (1)$$

Because the STB and GTB acquisitions are not fully synchronized, it is necessary to compute the coefficient over a rolling window to find its maximum and thus find the time-shift between the two series, as shown in Fig. 2. We chose a 180000 samples sliding window (over 200000 samples).

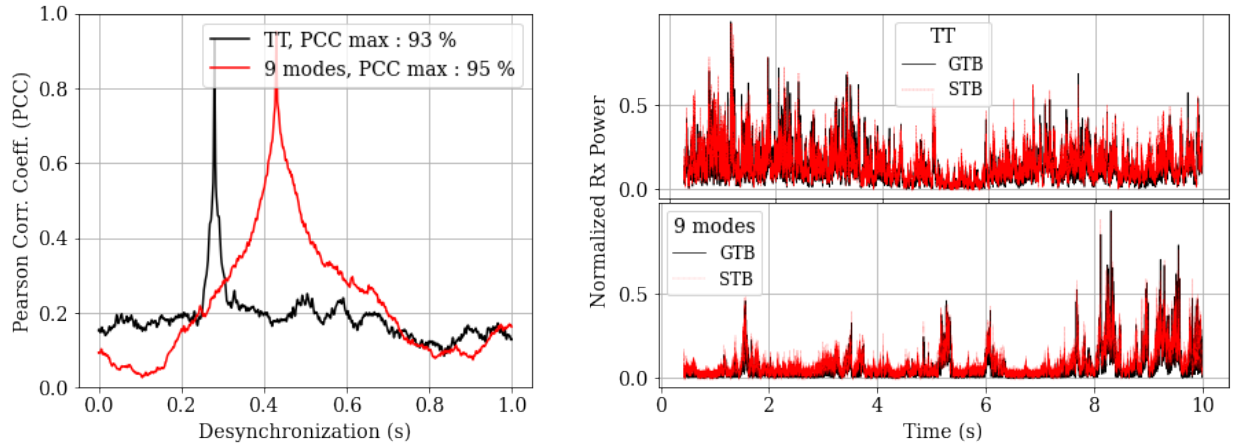


Fig. 2. On the left the PCC computed for a given desynchronization between the uplink and downlink acquisition, on the right the normalized and synchronized Rx and Tx power for the Tip-Tilt corrected signal and the 9 modes corrected signal. These results were obtained for the following integrated parameters : Fried parameter $r_0 = 8$ cm and the Rytov variance of the log-amplitude $\sigma_{\chi}^2 = 0.15$.

C. Upgrade of the reciprocity set-up

First measurements were done during the first campaign reaching 85% of signal correlation. Part of this correlation loss may be explained by the original set-up, composed with two different Rx/Tx pupils separated by $1.9 \mu\text{rad}$ angular distance on the STB module, hence leading to residual PAA anisoplanatism.

It was chosen to upgrade the experimental set-up for the second campaign so as to obtain a truly mono-axial scheme by means of a dedicated coupling system on-board the STB module, as shown in the STB part of Fig. 3.

Thanks to this new set-up, correlation results up to 95% were obtained. These results are presented in Fig. 2. The best correlation coefficient of 95% is obtained for the 9 modes correction, and the Tip-Tilt only correction gives a 93% correlation. We notice in this result a high latency between the two signals (0.5 s). This is due to the experimental architecture implying a variable desynchronization between the two time series acquisition. Computing the PCC is therefore a way to re-synchronize the two time series during the post-processing.

However, one could wonder what limits the effective reciprocity. The origin of the decorrelation is analysed and discussed in the following part.

IV. ANALYSIS OF THE EXPERIMENTAL RESULTS

A. Reciprocity principle and partial reciprocity of the bench

Let us first remind the principle of channel reciprocity. This principle states that if, in a given plane at one end of the link, the reception mode (Rx) and the laser emission mode (Tx) are equals and collocated, and if this statement actually applies at both ends, say in plane 1 and in plane 2 respectively, then the coupled flux in plane 2 (propagation from plane 1 to plane 2) and that in plane 1 (propagation from plane 2 to plane 1) are strictly equal.

In order to demonstrate this principle experimentally, we counter-propagate two laser beams between the STB and the

GTB along the same optical axis. The system geometry of the FEEDELIO experiment is depicted in Fig. 4. The system may seem asymmetrical, because of the different pupil size, of the different optical benches on the STB and GTB (that includes AO) and of the uneven distribution of turbulence on the line of sight. However, as in the GEO-Feeder case depicted in [12] [13], the property that ensures link reciprocity, related to the Rx/Tx mode symmetry, is verified.

Indeed, as shown on the sketch, the Tx/Rx modes at GTB are identical and correspond to the truncated Gaussian represented in red, and reciprocally, the Tx/Rx modes at STB are identical and correspond to the truncated Gaussian displayed in blue. To detail, the GTB emitted Gaussian mode, truncated by the 35 cm pupil, is focused towards the STB in this finite distance configuration. After propagation, only the top of this propagated (and distorted) beam is collected by the STB 1.8 mm collimator (few tens of times smaller than the received beam size) and then coupled to an SMF. Reciprocally, a truncated Gaussian mode is emitted from the STB. Due to the tiny 1.8 mm STB aperture, the beam strongly diverges, and, only its top is collected by the GTB 35 cm aperture and then coupled to the SMF.

However, although the reciprocity principle applies to this scheme, the link may become in practice only partially recip-

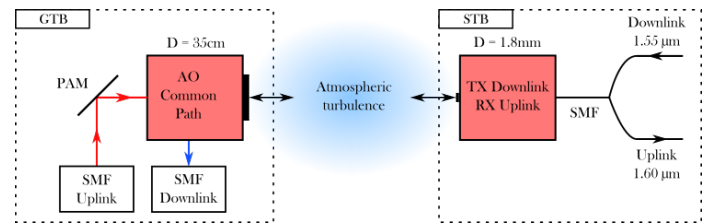


Fig. 3. Block diagram of the system. The black arrows represent the common path. The red arrows correspond to the uplink non common path after the mode emission and the blue arrows to the non common path of the downlink before coupling into a SMF.

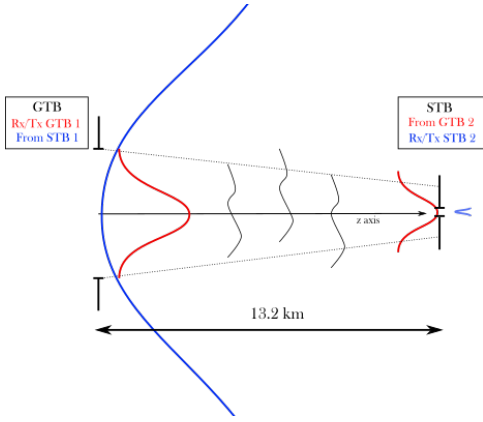


Fig. 4. Reciprocity scheme in the FEEDELIO geometry taking account of the finite distance of the line of sight. On the left in the GTB plane, the red mode is the Rx/Tx mode of the GTB and the blue mode is the one received from the STB. On the right, in the STB plane, the blue mode is the Rx/Tx mode of the STB and the red mode is the received mode from the GTB. We specify that the Tx mode from STB after propagation, in the GTB plane (in blue), is a wide Gaussian-like mode of which we represent only the top.

rocal because of the different light-paths taken by the uplink and the downlink in the GTB module. As shown in Fig. 3, the different paths taken may introduce NCPAs of the first order due to the PAM pointing mirror which has a limited repeatability around $1 \mu\text{rad}$, and of higher orders aberrations due to other differential optical elements on the bench.

In this next part, by means of numerical simulations, we quantify the reciprocity loss that is introduced by specific NCPAs.

B. Impact of NCPAs on the decorrelation

1) *NCPAs sources and measurements on the bench:* The first source of NCPAs is due to the PAM on the uplink path. Indeed this mirror is necessary to adjust the pointing towards the STB module. It was observed that the mispointing error induced by the PAM repeatability was in the order of $1 \mu\text{rad}$ which corresponds to a value of approximately 0.7 rad of Zernike Tip-Tilt coefficient. This repeatability error was due to changes of temperature as well as vibrations.

TABLE I
TABLE OF THE NCPAs MEASURED ON THE OPTICAL BENCH

| | Aberration type (rad) | | | | |
|------------|-----------------------|-------|-------|-------|--|
| | a_2 and a_3 | a_4 | a_5 | a_6 | |
| Downlink | 0 | 0.4 | 0 | -0.1 | |
| Uplink | [-0.35,0.35] | 0.4 | 0.3 | -0.1 | |
| Common | | × | | × | |
| Non Common | × | | × | | |

We then measured the higher order aberrations, reported on the table I. These measurements consist in optimizing the received coupled flux (emitted from internal source), by varying the reference phase of the AO loop, on the uplink path and on the downlink path. It was found that there is a_5 differential astigmatism between the two lightpaths. We also measured defocus and a_6 astigmatism, but these aberrations

were common and thus corrected by the AO loop on both paths.

2) *Numerical simulation framework:* The objective here is to compare the experimental results with numerical simulation results to investigate the origin of the decorrelation of the signal. In this purpose, we used an in-house E2E numerical model, described in [14], based on Monte-Carlo simulation in a spherical wave propagation mode. To have an accurate analysis, we use the Cn2 profile reconstructed from the studied time series.

After generation of the downlink perturbed complex fields time series, we use an AO system numerical model to simulate different types of correction. The number of corrected equivalent Zernike modes is tuned from 2 (Tip-Tilt) to 35 (full correction). This set of complex fields corresponds to the downlink reference $\{\Psi_{\text{Down},i}(\mathbf{r})\}_{i=0, N_{\text{Samples}}}$.

The simulation exploits channel reciprocity. Coupling of both downlink and uplink are therefore calculated in the GTB aperture. For downlink we compute an overlap integral between the plain complex field $\Psi_{\text{Down}}(\mathbf{r})$ and the GTB Rx mode. For uplink, before computing the overlap integral, we apply NCPAs to $\Psi_{\text{Down}}(\mathbf{r})$, that can be considered as a reciprocal uplink complex field [13]. The NCPA wavefront is expressed as a sum of weighted Zernike polynomials :

$$\Phi_{\text{Aberrated}}(\mathbf{r}) = \sum_{i=2}^{N_{\text{NCPA}}} a_i Z_i(\mathbf{r}) \quad (2)$$

with N_{NCPA} the maximum order of measured NCPAs, a_i the aberration associated to the i^{th} Zernike coefficient Z_i in radian.

These wavefronts are applied to the original downlink field as :

$$\Psi_{\text{Up},i}(\mathbf{r}) = \Psi_{\text{Down},i}(\mathbf{r}) \cdot \exp(j\Phi_{\text{Aberrated}}(\mathbf{r})) \quad (3)$$

with i the sample number, \mathbf{r} the spatial vector coordinates.

We then compute the overlap integral between the field and the reception gaussian mode of the fiber for each of the two fields and then deduce the respective coupled flux. The PCC is computed from the two resulting time series.

3) *Comparison to simulation results:* The aim here is to explain the two effects that can be seen on Fig. 2. Firstly, we observe that it remains at least 5% of decorrelation between the two experimental signals in a 9 modes correction scheme. Secondly, there is a 2% decorrelation difference between the 2 modes correction and 9 modes correction. Knowing the pointing imprecision and the measured NCPAs on the bench, the following numerical simulations will help quantifying the impact of such aberrations on the signals decorrelation and though on the link reciprocity.

In the following study, we first analyse separately the impact of the mispointing, which corresponds to the Tip-Tilt error (1st order NCPAs) and of astigmatism (Higher order NCPAs), in a given spatial direction. We then analyse the combined effect of these two aberrations.

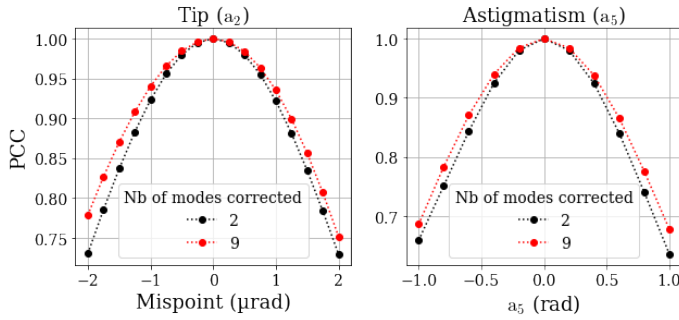


Fig. 5. Computation of the PCC for two time series deduced from a reference field and an aberrated field with additional NCPAs. The left curves depicts the sensitivity to additional Tip (a_2) in the range -0.7 rad to 0.7 rad, corresponding to a horizontal mispointing of -2 μ rad to 2 μ rad. On the right is depicted the sensitivity to a non common astigmatism in the range from -1 rad to 1 rad.

We can observe on the left curve in Fig. 5 a fast decorrelation with a growing mispointing, while correlation values are of the same order of magnitude as the one observed on the experimental signal. The same phenomenon can be observed with the astigmatism (on the right). Moreover, we can also observe that the Tip-Tilt only corrected signal is more sensitive to the mispointing than the 9 modes corrected signal.

We then analyse the combined effect of a mispointing added to 0.3 rad of astigmatism as measured on the bench. We study two cases : one with a_5 astigmatism and one with a_6 astigmatism, to take account of some potential relative orientation effects (given that we only explore the horizontal mispointing direction). The results depicted in Fig. 6 show that, in both simulations, one can find a mispoint value providing correlation values similar to the experimental ones (93% and 95% for 2, respectively 9, corrected modes). The

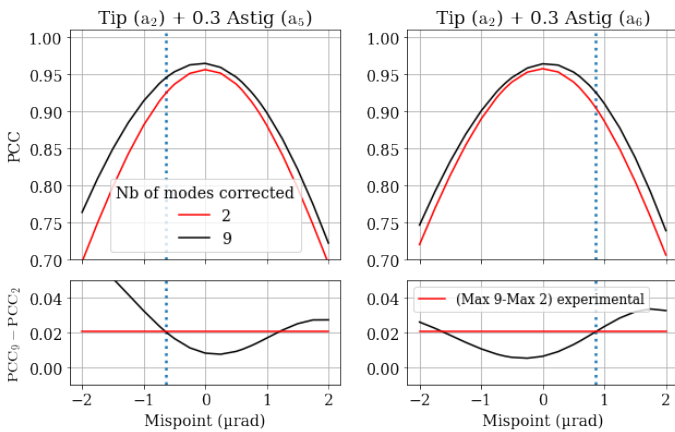


Fig. 6. Computation of the PCC for two time series deduced from a reference field and an aberrated field with additional NCPAs. The range of imposed Tip is -0.7 rad to 0.7 rad, corresponding to a horizontal mispointing of -2 μ rad to 2 μ rad. Furthermore, a constant astigmatism of 0.3 rad is added. The figures at the bottom correspond to the difference between the 9 modes and the 2 modes curves (black), and the red line is the difference between the experimental correlations for these 2 correction orders.

values obtained are consistent with the error due to pointing mirror repeatability, although close to the bounds of plausible mispointing values.

C. Sensitivity to the optical correction

Furthermore, beyond the low order modes correction behavior noticed in Fig. 2 and Fig. 6, it was noticed in a second experimental acquisition that the correlation was even more degraded for a higher number of modes corrected and thus a better quality of correction. Indeed, it can be observed in experimental results that the PCC reaches a peak for a 9 modes correction and then decreases for the AO full correction mode (equivalent to around 35 Zernike modes corrected).

Starting from the data simulated in IV-B3, we investigated the impact of different AO corrections (from Tip-Tilt to 45 modes) on the decorrelation. We added to the resulting fields the same static Astigmatism a_5 of 0.3 rad and tuned the Tip and Tilt values. Figure 7 shows decorrelation given a number of AO corrected modes, for one set of such NCPAs. As noticed on experimental data, we observe a decrease of the correlation for high order correction. We believe that since high order correction leads to a sharper beam on the STB plane, it leads therefore to higher sensitivity to NCPAs and particularly to mispointing. We still pursue data processing and numerical analysis of this effects.

D. Discussion about the use of the reciprocity for calibration purposes

Beyond the analysis of the partial reciprocity observed experimentally, one can discuss how can the reciprocity experiment be exploited. The first application would be for calibration purposes, be it for slant path demonstrators as FEDELIO or VERTIGO [15], or to test equipment intended to be integrated in ground stations for further ground to satellite optical links. In that sense, optimizing the reciprocity can be a method to minimize the NCPAs of the optical bench. This procedure can also be used in the scope of horizontal

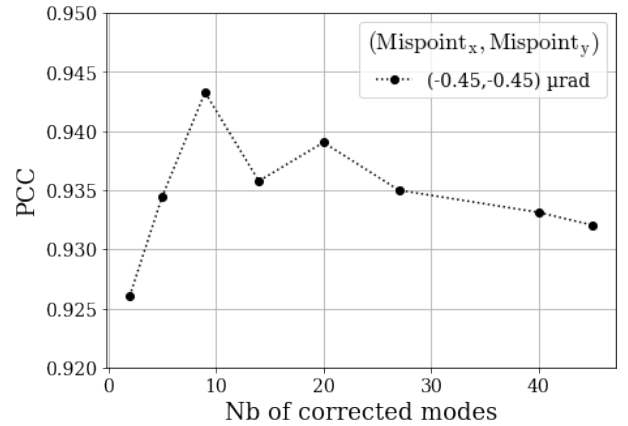


Fig. 7. Study of the decorrelation sensitivity to the number of AO modes corrected. The black curve corresponds to the PCC issued from the simulation. The simulation operating point is a mispointing in both x and y direction of $(-0.45, -0.45)$ μ rad and 0.3 rad a_5 astigmatism.

FSO links, for calibration but also to provide, as recalled in the introduction, channel state information and thus improve the digital signal processing. Furthermore, it can be added that, although partial due to angular decorrelation, this channel state information can also be exploited in the ground-to-satellite optical links framework.

It is also noticeable that such a reciprocity concept can be used at the numerical simulation level, both for E2E simulations and pseudo-analytical simulations. For instance, in the analysis of phenomenon such as point-ahead anisoplanatism, using a reciprocal approach gives access to information not provided by classical E2E simulation for uplink optical signals, as depicted in [13]. Concerning pseudo-analytical simulation, this paradigm can also be used to simulate the uplink and reduce the computation cost [12].

V. CONCLUSION

To conclude, we performed in the frame of the FEEDELIO measurement campaign a reciprocity experiment that was fruitful. We interpreted the results obtained thanks to numerical simulations themselves relying on the reciprocity principle. Simulations showed that the experimental decorrelations can be explained by the presence of NCPAs (mispointing and astigmatism) on the optical set-up. Moreover, we explored the decorrelation induced by different AO correction orders. This analysis assesses the FEEDELIO set-up quality and stresses the need for high precision performance evaluation tools for in-depth understanding of the data.

We recall that further analysis of the FEEDELIO results will soon be published in [2]. These results will emphasize on the AO pre-compensation effectiveness in presence of angular anisoplanatism on a statistical point of view. A deeper analysis of both first and second campaign results will then be conducted with an emphasis on the uplink signal temporal signature.

ACKNOWLEDGMENT

This work has been performed in the framework of ESA's contract N°4000120300/17/NL/PS. FEEDELIO experiment could not have been possible without the very helpful contributions of the technical staff from Instituto Astrofísica de Canarias, Teide's National Park and Teide's cable car station. The author warmly thank them for their fruitful help and collaboration.

In addition, part of this work has been performed in the framework of a PhD funded by CNES and ONERA. We thank the CNES supervisors Bouchra Benammar and Hugo Meric, and the PhD advisor Ghaya Rekaya from Telecom Paris for their advice.

REFERENCES

[1] N. Védrenne, A. Montmerle-Bonnefois, C. B. Lim, C. Petit, J.-F. Sauvage, S. Meimon, P. Perrault, F. Mendez, B. Fleury, J. Montri, J.-M. Conan, V. Michau, Z. Sodnik, and C. Volland, "First experimental demonstration of adaptive optics pre-compensation for geo feeder links in a relevant environment," in *2019 IEEE International Conference on Space Optical Systems and Applications (ICSOS)*, pp. 1–5, 2019.

[2] A. M. Bonnefois, M.-T. Velluet, M. Cissé, C. B. Lim, J.-M. Conan, C. Petit, J.-F. Sauvage, S. Meimon, P. Perrault, F. Mendez, B. Fleury, J. Montri, V. Michau, and N. Védrenne, "First feasibility demonstration of ao pre-compensation for geo feeder links in a relevant environment." to be published.

[3] J. H. Shapiro, "Reciprocity of the turbulent atmosphere*," *J. Opt. Soc. Am.*, vol. 61, pp. 492–495, Apr 1971.

[4] D. Giggenbach, W. Cowley, K. Grant, and N. Perlot, "Experimental verification of the limits of optical channel intensity reciprocity," *Appl. Opt.*, vol. 51, pp. 3145–3152, Jun 2012.

[5] R. R. Parenti, J. M. Roth, J. H. Shapiro, F. G. Walther, and J. A. Greco, "Experimental observations of channel reciprocity in single-mode free-space optical links," *Opt. Express*, vol. 20, pp. 21635–21644, Sep 2012.

[6] S. Parthasarathy, D. Giggenbach, C. Fuchs, R. Mata-Calvo, R. Barrios, and A. Kirstaedter, "Verification of channel reciprocity in long-range turbulent fso links," in *Photonic Networks; 19th ITG-Symposium*, pp. 1–6, 2018.

[7] N. Védrenne, J.-M. Conan, A. Bonnefois, C. Petit, M.-T. Velluet, and V. Michau, "Adaptive optics pre-compensation for geo feeder links: Towards an experimental demonstration," in *2017 IEEE International Conference on Space Optical Systems and Applications (ICSOS)*, pp. 77–81, 2017.

[8] A. M. Bonnefois, J. M. Conan, C. Petit, C. B. Lim, V. Michau, S. Meimon, P. Perrault, F. Mendez, B. Fleury, J. Montri, and N. Védrenne, "Adaptive optics pre-compensation for GEO feeder links: the FEEDELIO experiment," in *International Conference on Space Optics — ICSSO 2018* (Z. Sodnik, N. Karafolas, and B. Cugny, eds.), vol. 11180, pp. 889 – 896, International Society for Optics and Photonics, SPIE, 2019.

[9] N. Védrenne, V. Michau, C. Robert, and J.-M. Conan, "Cn2 profile measurement from shack-hartmann data," *Opt. Lett.*, vol. 32, pp. 2659–2661, Sep 2007.

[10] C. Robert, J.-M. Conan, V. Michau, J.-B. Renard, C. Robert, and F. Dalaudier, "Retrieving parameters of the anisotropic refractive index fluctuations spectrum in the stratosphere from balloon-borne observations of stellar scintillation," *J. Opt. Soc. Am. A*, vol. 25, pp. 379–393, Feb 2008.

[11] K. Pearson, "Note on Regression and Inheritance in the Case of Two Parents," *Proceedings of the Royal Society of London Series I*, vol. 58, pp. 240–242, Jan. 1895.

[12] J.-M. Conan, A. Montmerle-Bonnefois, N. Védrenne, C. B. Lim, C. Petit, V. Michau, M.-T. Velluet, J.-F. Sauvage, S. Meimon, C. Robert, J. Montri, F. Mendez, P. Perrault, G. Artaud, and B. Benammar, "Adaptive Optics for GEO-Feeder Links: from Performance Analysis via Reciprocity Based Models to Experimental Demonstration," in *COAT-2019 - workshop (Communications and Observations through Atmospheric Turbulence: characterization and mitigation)*, (Châtillon, France), ONERA, Dec. 2019.

[13] C. Robert, J.-M. Conan, and P. Wolf, "Impact of turbulence on high-precision ground-satellite frequency transfer with two-way coherent optical links," *Phys. Rev. A*, vol. 93, p. 033860, Mar 2016.

[14] N. Védrenne, M.-T. Velluet, C. Petit, V. Michau, J. Chabé, A. Ziad, D.-H. Phung, N. Maurice, E. Samain, G. Artaud, J.-L. Issler, M. Toyoshima, M. Akioka, D. Kolev, Y. Munemasa, H. Takenaka, and N. Iwakiri, "First results of Wavefront sensing on SOTA," in *2015 IEEE International Conference on Space Optical Systems and Applications (ICSOS)*, pp. 1–8, 2015.

[15] A. L. Kernec, L. Canuet, A. Maho, M. Sotom, D. Matter, L. Francou, J. Edmunds, M. Welch, E. Kehayas, N. Perlot, M. Krzyzek, A. Paraskevopoulos, J. Leuthold, Y. Horst, J. Bourderionnet, A. Brignon, E. Lallier, V. Billault, L. Leviandier, J.-M. Conan, N. Védrenne, C. B. Lim, A. Montmerle-Bonnefois, C. Petit, L. Stampoulidis, M. Fehrenz, and T. Lehnigk-Emden, "The H2020 VERTIGO project towards tbit/s optical feeder links," in *International Conference on Space Optics — ICSSO 2020* (B. Cugny, Z. Sodnik, and N. Karafolas, eds.), vol. 11852, pp. 508 – 519, International Society for Optics and Photonics, SPIE, 2021.